USING EXTERNAL HIGH-RESOLUTION LOG SCANNING TO DETERMINE INTERNAL DEFECT CHARACTERISTICS

Ed Thomas, Liya Thomas, Clifford Shaffer, and Lamine Mili

Research Scientist, Northeastern Research Station, 241 Mercer Springs Road, Princeton, WV 24740; PhD. Student, Department of Computer Science, Virginia Tech, Blacksburg, VA 24061; Associate Professor, Department of Computer Science, Virginia Tech, Blacksburg, VA 24061; Professor, Bradley Department of Electrical and Computer Engineering, Virginia Tech, Alexandria Research Institute, Alexandria, VA 22314

Abstract--The location, type, and severity of external defects on hardwood logs and stems are the primary indicators of overall log quality and value. External defects provide clues about internal log characteristics. More than 1,000 yellow-poplar defect samples have been collected to establish an external/internal defect databank. There are strong correlations among external indicators and internal features have been discovered. The ability to determine the location and characteristics of internal log defects in real-time should improve the lumber production dramatically with respect to quality and quantity. A high-resolution laser log scanner was used to scan 162 red oak and yellow-poplar logs. The processed laser images show most bark texture features and surface characteristics of the original log or stem. Defects with height differentiation from the background log surface are distinguished using the contour levels of a residual image. Simple shape definition rules combined with the height map allows detection of the most severe defects.

INTRODUCTION

Traditionally, before a hardwood log is processed it undergoes a subjective (visual) assessment, typically by a mill operator. The difference between high and low quality logs is determined by defect type, frequency, size, and location. It is difficult to accurately and rapidly detect and measure defects, either mechanically or manually (Tian and Murphy 1997). For every surface indicator there is usually an associated internal defect. External defect indicators are bumps, splits, holes, and circular distortions in the bark pattern. Bumps usually indicate overgrown knots, branches, or wounds. Some bumps have a cavity or hole in the middle, indicating that the overgrown material has decay or is rotten. Circular distortions, or rings around a central flattened area, indicate a branch that was overgrown many years earlier. Surface defects progress from a pruned or broken branch to an overgrown

knot characterized by a significant bump and then to a rotten knot or a distortion defect. For some classes of defects, it is possible to accurately predict internal features based on external characteristics.

Studies have demonstrated that the use of external or internal defect data improves cutting strategies that optimize log recovery or yield, i.e., preserving the largest possible area of clear wood on a board face (Steele et al. 1994). The value of the lumber that can be recovered depends on the presence and location of defects. This is especially true for hardwood logs. In the production of hardwood lumber, boards are sawn to fixed thicknesses and random widths. The presence and placement of defects on the boards affect board quality and value, so much attention is focused on log surface defects during processing.

Several scanning and optimization systems are available that aid in the sawing of logs into lumber. Two types of defect detection are used on hardwood logs: internal and external. Various internal defect inspection methods have been proposed in the literature based on X-ray/CT (Computer Tomography), X-ray tomosynthesis, MRI (magnetic resonance imaging), microwave scanning, ultrasound, and enhanced pattern recognition of regular X-ray images (Guddanti and Chang 1998; Schmoldt 1996; Wagner et al. 1989; Zhu et al. 1991). CT and MRI systems provide excellent internal images of logs, but image acquisition is slow and expensive and variable moisture content and log size can present problems to the CT scanning device (Bhandakar et al. 1999). Currently, there is no known commercial installation of these methods.

Laser-line scanners are commonly used in sawmills to gather information on external log characteristics, e.g., diameter, taper, curvature, and length (Samson 1993). Optimization systems use the laser-profile information to better position the log on the carriage and improve the sawyer's decision-making ability. These systems typically were developed for softwood, e.g., pine, spruce, fir log processing. They are becoming increasingly commonplace in hardwood mills as well.

Our research takes the three-dimensional log surface image and processes it to determine the location of the most severe external defects: overgrown knots, rotten knots, holes/gouges, and removed branches. These types of defects usually are associated with a significant surface rise or depression depending on the defect type. The image is processed using a robust statistical approach to generate a height map of the log. Defects are characterized and located by a height change from the surrounding log area. Many internal aspects of the defect can be

predicted. This system is currently under development and is expected to permit an inexpensive, automated approach to determining interior defect information.

THE INTERNAL/EXTERNAL DEFECT RELATIONSHIP

The Logger Databank is an unpublished USDA Forest Service database containing more than 20,000 logs of various hardwood species collected over a 40 year period by the Forest Products Laboratory and Northeastern Research Station. The databank contains size and location information for all side and end defect indicators. We used the databank to construct a random sample of approximately 33% of the total yellow-poplar (*Tulipifera liriodendron*) defect population. For log grades 1, 2, and 3, 80% of all defects are in nine defect types. According to the log grading rules the following log surface abnormalities are serious grading defects that lower quality and strength: bulges, bumps, burl, conk, holes, knots (sound, unsound, and overgrown), insect damage, bark distortions, pin, shot, spot, and flagworm holes (Ostrander 1965). Overlaying this information with defect population data, we determined the defect types that should be sampled from the forest.

Two sites in West Virginia were selected for defect sample collection: West Virginia University Forest (WVUF) near Morgantown (elevation: 2300 feet) and Camp Creek State Forest (CCSF) near Princeton (elevation: 2600 feet). The two sites are separated by 220 miles. The number of defects obtained from each site by defect type is shown in Table 1. In most cases, approximately equal numbers of each type of defect were obtained from each site. The exceptions are the light distortion (LD) and unsound knot (UK) defects. We did not collect LD defects from the WVUF. UK defects occured in much fewer numbers at CCSF than at WVUF. Thirty-three yellow-poplar trees were selected randomly from each site. From each tree the number of defects of each type was counted and recorded. Random numbers were used to select which defects to choose from each tree. The goal was to select three or four defects of each type available from each tree. The placement of defects on the tree often meant choosing one to the exclusion of others.

For each defect sample, the diameter of the log inside the bark, bark thickness, and ring count are recorded. An alignment groove is milled into the top of the sample to indicate orientation and to provide a measurement point for calculating the penetration angle of the defect. Next, each sample was sliced into 1-inch-thick slabs. On the surface and for each slab the defect width, length, and distance from defect

center to the bottom center of the alignment groove are measured as is the height of the defect on the surface also is measured. A series of defect slabs is shown in Figure 1.

Methods

Using SYSTAT (Wilkinson 1988) a series of linear regression analyses were performed on the exterior/interior data series. The independent variables included: defect surface width, surface length, surface height, diameter, height above ground, and growth rate. Although height above ground and growth rate usually would not be known when examining a given log, we included these variables to determine the effect if any on predicting internal characteristics. The dependent variables are clear-area-above-defect (thickness of usable wood above an encapsulated defect), penetration angle, total depth, halfway in width, and length.

Each defect type was analyzed separately. A stepwise function ($p > 0.15$) was used to identify significant variables; the linear regression package was used to identify outliers. The outliers were examined to determine whether the data could be corrected (data entry error) before exclusion. In all cases, the number of outliers removed from each defect class was less than 7% of each defect-class population.

Results

Surface features for most defects generally are correlated with internal features. The results from the stepwise multiple linear regression analyses are presented in Table 2. R^2 values were best with the most severe defect types. For sound, unsound, and overgrown knots, the models were effective in predicting total penetration depth of the defect and the cross-section dimensions at the midway penetration point. Another perhaps more important factor is the low mean absolute error (MAE). Even with slightly low R^2 values, the error is sufficiently low to allow a somewhat accurate prediction of internal features. For example, the MAE for overgrown knots is 0.240 inch. Thus, the regression model predicts a size that is on average within ±0.240 inch of the actual size.

For less severe defects, heavy, medium, and light distortions, total depth continues to be highly correlated with surface features and has a low MAE. However, the halfway-in-width and length are not as strongly correlated with surface features as with the more severe defects. A low MAE likely will allow prediction of internal features sufficient for grade recovery optimization. This assumption will be tested in future research.

Adventitious knots and adventitious knot clusters also were examined, but most internal features were not strongly correlated with exterior features. The results of these analyses have been omitted from Table 2. One may observe from this that the less severe the defect, the less correlation the internal features have with the external indicators. This may be due to longer encapsulation time (i.e., time since defect began to be overgrown by good wood) that has obscured external indicators.

Rake or penetration angle is not as well correlated to surface features as other internal features for all defect types. In the rake model, growth rate appeared as a significant variable. It was omitted from these results as it is not immediately discerned from a surface examination of the log. For the distortion defects, no surface variables were significantly correlated to rake. Rake angle is approximately normally distributed with a mean of 21.87 and a standard deviation of 11.03, so it may be possible to use these values for the placement of the internal defect. This possibility needs to be tested to discern how sensitive grade recovery is to the variable placement of the defect with respect to penetration angle.

LASER LOG SCANNING TO DETECT EXTERNAL DEFECTS

We used a portable demonstration laser log scanner to collect log surface data http://www.usnr.com/perceptron/products.htm. The scanner had four laser-line generator/camera units stationed at 90-degree intervals around the log's circumference. Triangulation was used to determine locations of log surface points covered by the laser line. A combination of 162 northern red oak (*Quercus rubra*) and yellow-poplar (*Tulipifera liriodendron*) logs was scanned. These are two of the most common and important commercial species in the Eastern United States. The sample of logs scanned was obtained both from the forest and from local sawmills. In general, logs from the forest are in better condition than those from sawmills due to less handling. Also, forest logs have less damage with fewer and smaller areas of missing bark than mill logs.

The log scanner recorded a laser line measurement approximately every 0.78 inch along the logs length. A transducer records the lineal position of the scanner accurate to 0.01 inch. The data set shown in Figure 2 consists of 1,290 three-dimensional Cartesian coordinates in a single plane or "cross section." The average distance between points in each cross section is 0.04 inch. When a sequence of cross sections is

assembled, a three-dimensional map of the log surface is obtained. Using OpenGL (a 3D programming data display environment), realistic views of the scanned log surfaces (Fig. 3) are rendered that are useful for visually examining log surfaces and defect characteristics.

Data Processing

To convert the 3-D log surface data to 2-D images for processing, a reference surface must be imposed on the log data. Since logs are natural objects that are approximately circular or elliptical in cross section, we fit circles or ellipses to the log data, which together form a reference surface. Defects that correspond to rises or depressions on the log surface can be detected using contour levels estimated from the orthogonal distances between the reference surface and any point of the cross section.

Fitting quadratic curves (i.e., circles, ellipses) to 2-D data points is a nonlinear regression problem (Gander et al. 1994). Classic least-squares fitting methods failed because the laser log cross-section data contain missing data and/or large deviant data points. In robust statistics, outliers are defined as data points that strongly deviate from the pattern formed by the majority of the measurements. The laser data sets include outliers generated by dangling loose bark, duplicate and/or missing data caused by scanner calibration errors, unwanted data from the supporting structure under the log, and missing data due to the blockage of the log by the supporting structure. To overcome the non-robustness of the least-square fitting, we resorted to the theories and methods of robust statistics (Hampel et al. 1986). The nonlinear form of the circle equation prompted us to develop a new robust estimation method that is an outgrowth of the one proposed by Mili et al. (1996).

Our nonlinear regression circle-fitting estimator is a generalized M-Estimator, termed GM-estimator (Thomas et al. 2004). It not only filters the errors in the measurements but also the errors in the circle model that are applied to a given cross-sectional data set. For a log sample with 120 cross sections, an equal number of circles are fitted, forming a reference surface for the residual extraction. Unlike the method described in Mili et al. (1996), our estimator minimizes an objective function that uses a weight function that levels off for large scaled radial distance between the associated data point and the fitted circle; it does this at every step of the iterative algorithm that solves the estimator. We tested the robustness of our estimator on real log data samples and found that the resulting fitted circles vary little

among neighboring cross sections, yielding a smooth fit over the entire data of a log.

Defect Detection

The next step is to convert the three-dimensional, laser-scanned Cartesian coordinates into a two-dimensional, 256 gray-level image (Fig. 4). In this process, the log surface is unrolled onto a 2-D coordinate space. In essence, this process creates a "skin" of the log surface representing the pattern of the log's bark along with the bumps and bulges associated with most defects. Using the adjusted, fitted circle to each cross section, we calculate the radial distances between circle and log surface points, typically ranging from -0.5 to 0.5 inch. The radial distances are scaled to range from 0 to 255 and mapped to gray-levels to create a 2-D image. Originally the log data are not in a grid format. As a result they are processed and interpolated linearly to fill any gaps between data points.

To detect defects, we developed an expert system to accommodate the many possible defect sizes, heights, shapes, types, etc. The main method incorporated in the algorithm is identifying defect areas via a series of elimination of non-defective areas among many potential candidates. This is achieved by using measured and processed log data (converted for the defect detection algorithm), expert knowledge, and expertise in a stepwise fashion. The data resolution (0.8 inch per cross section) and the nature of external defect shapes restrict search scope in the algorithm.

Two major steps are involved in the defect detection algorithm. The first step consists of finding the most obvious defects and their external characteristics, including protrusion on surface, certain width-length ratio, area size. Shape and characteristics were obtained from the samples collected for modeling the external/internal defect relationship.

Because most severe defects have a localized height change, a height analysis of the residual image provides information on the presence of severe defects. A substantial, localized, and abrupt surface rise or depression greater than 1.0 inch is almost always a defect. Since the pixel values in the gray-level image represent radial distances between the fitted circle and the log surface, the analysis is straightforward. Using the gray-level image (Fig. 4) we generate a contour plot as depicted in Figure 5. In the contour plot image, it is possible to discern areas containing likely defects based on height information alone. We developed an algorithm to generate the rectangles that enclose

areas within a contour curve at the highest level. The areas are selected depending on their sizes, five of the six surface defects were found using this method. Figure 5 also presents a manually recorded map of the defects on the same log. The defect types represented in the map include SKs (sound knots), OKs (overgrown knots), and a gouge. A type of hole defect, a gouge is an area of missing wood usually created during felling or poor handling.

Certain defects, particularly sawn knots, often are partially detected in the contour because they are relatively low-lying and flat. Thus, only a corner is enclosed in the highest contour. The second step of our algorithm uses a statistical expert system to examine the area surrounding such a small region for relatively straight-line segments. If the coverage of straight-line segments is sufficient, the defect area is adjusted to cover the entire defect surface rather than just a corner.

Results

In the first step of our algorithm, the most severe and obvious defects are identified. They have a relatively significant height change on the surface (• 0.5 inch) and/or a relatively significant size (• 3 in. in diameter). We refer to such defects as "expected to be detected," while the others are termed "unexpected to be detected" (Table 3). We use this grouping because the log-data resolution, 0.8 inch per cross section, is not high enough to clearly detect defects whose diameters are smaller than 3 inches. In addition, the current version of our system uses the contour image generated from the radial distances that provide a map of defect height change against the surrounding bark. For certain classes of defects, our detection algorithm has a probability of detection of 81% (48 of 59) for the most serious defect classes. Further, it has a 36% detection rate for all defects and 19% false detection rate (14 of 73 identified defects).

DISCUSSION

Due to the presence of extreme outliers and missing data in the laser log data, robust estimation techniques are well suited to this application. The developed programs can process an entire log-data sample by transforming the original log data set, which may contain a large number of missing and/or severe deviant data, into a sharper and cleaner image. The quality of the resulting gray-level image lays a solid foundation for the remaining defect-detection process. Contour levels derived from the residuals allowed us to detect and further narrow the potential defect areas.

The laser-log scanning system is effective in locating severe defect types. The external scanning system determines the diameter of the log at the defect and the width, length, and rise (if any) of the surface indicator. These variables are required input to the external/internal defect modeling system. We are working to combine the two systems to provide a simulated external whole log scanner that infers knowledge of internal defect structures based on external indicators. Additional enhancements to the system will require a laser scanner with an increased longitudinal resolution (0.1 inch between cross sections). Such scanners are currently available and would allow texture-based approaches to finding defects without a significant surface rise. Also we may be able to correlate aspects of the surface texture with internal features, thereby improving the model's predictive power for less severe defects.

LITERATURE CITED

Bhandakar, S.M., T.D. Faust, and M. Tang, 1999. CATALOG: a system for detection and rendering of internal log defects using computer tomography. Machine Vision and Appl. Springer-Verlag. 11: 171-190.

Gander, W., G.H Golub, and R. Strebel. 1994. Fitting of circles and ellipses—least squares solution. Tech. Rep. 217. Insitiut fur Eisenschaftliches Rechnen, ETH Zurich. ftp://ftp.inf.ethz.ch/doc/tech-reports/2xx/ .

Guddanti, S. and S.J. Chang. 1998. Replicating sawmill sawing with TOPSAW using CT images of a full length hardwood log. For. Prod. J. 48(1):72-75.

Hampel, F.R., E.M. Ronchetti, P.J. Rousseeuw, and W.A. Stahel. 1986. Robust statistics: The approach based on influence functions. John Wiley, New York.

Mili, L., M.G. Cheniae, N.S. Vichare, and P.J. Rousseeuw. 1996. Robust state estimation based on projection statistics. IEEE Trans. on Power Systems. Vol. 11. No. 2.

Ostrander, M.D. 1965. A guide to hardwood log grading (Revised). U.S. Forest Service, Northeast Forest Experiment Station. Upper Darby, PA. 50 pp.

Samson, M. 1993. Method for assessing the effect of knots in the conversion of logs into structural lumber. Wood and Fiber Sci. 25(3):298-304.

Schmoldt, D.L. 1996. CT imaging, data reduction, and visualization of hardwood logs. In D. Meyer (Ed.) Proc. of the 1996 Hardwood Res. Symp. National Hardwood Lumber Association, Memphis, TN.

Steele, Phillip H., T.E.G. Harless, F. Wagner, L. Kumar, F.W. Taylor. 1994. Increased lumber value from optimum orientation of internal defects with respect to sawing pattern in hardwood sawlogs. For. Prod. J. 44(3):69-72.

Thomas, L., L. Mili, C. A. Shaffer, and E. Thomas. 2004. Defect detection on hardwood logs using high resolution three-dimensional laser scan data, *IEEE ICIP 2004,* Singapore. pp. 243-246.

Tian, X. and G.E. Murphy. 1997. Detection of trimmed and occluded branches of harvested tree stems using texture analysis. Int. J. of For. Eng.8(2):65-78.

Wagner, F.G., F.W. Taylor, D.S. Ladd, C.W. McMillin, and F.L. Roder. 1989. Ultrafast CT scanning of an oak log for internal defects. For. Prod. J. 39(11/12):62-64.

Wilkinson, Leland. 1988. SYSTAT: The system for statistics. SYSTAT, Inc. Evanston, IL.

Zhu, D., R. Conners, F. Lamb, and P. Araman. 1991. A computer vision system for locating and identifying internal log defects using CT imagery. Proc. of the 4th Int. Conf. on Scanning Tech. in the Wood Ind., Miller Freeman Publishing, Inc., San Francisco, CA: pp:1-13.

TABLE AND FIGURE CAPTIONS

Table 1.—Types and numbers of defects collected by site and overall
Table 2.—Correlation results for yellow-poplar samples by defect type
Table 3.–Statistics of the simulation of our defect detection system

Figure 1.—Photo series showing processed defect sample

Figure 2.—A data cross-section representing the circumference of a log on a 2-D plane

Figure 3.–OpenGL rendered image of the laser scanned log data

Figure 4.–Radial residuals generated by the log-unrolling process presented as a gray-level image. Light pixels represent protrusions from the log surface; dark pixels represent depressions. This log is approximately 9 feet long with a diameter of 2 feet.

Figure 5.—Left: Computer generated contour plot of a log surface with the four most obvious defect areas marked with crossed rectangles labeled in the descending order of area size. Right: Defect diagram illustrating the "ground truth." Note that only five small and/or flat defects were not detected.

Table 1.—Types and numbers of defects collected by site and overall

Defect	Location		Total
	CCSF	WVU Forest	
Adventitious knot (AK)	76	76	152
Adventitious knot cluster (AKC)	59	68	127
Bump (BUMP)	3	1	4
Heavy distortion (HD)	74	58	132
Light distortion (LD)	**96**	**6**	**102**
Medium distortion (MD)	87	80	167
Overgrown knot (OK)	89	79	168
Overgrown knot cluster (OKC)	**20**	**1**	**21**
Sound knot (SK)	47	46	93
Sound knot cluster (SKC)	2	0	2
Unsound knot (UK)	**7**	**33**	**40**
Wound (WND)	14	13	27
Total	574	461	1035

Table 2.—Correlation results for yellow-poplar samples by defect type

Defect	Dependent variable	Independent variables	Adjusted squared multiple R	Mean absolute error
Sound knot	Halfway-in length	Surface length, DIB	0.823	0.395 - inch
	Halfway-in width	Surface length, DIB	0.811	0.242 - inch
	Rake angle	Surface length, rise, DIB	0.640	10.90 - degrees
	Total Depth	Surface length, DIB	0.510	0.544 - inch
Unsound knot	Halfway-in length	Surface length, DIB	0.672	0.527 - inch
	Halfway-in width	Surface length	0.647	0.312 - inch
	Rake angle	Surface length, DIB	0.341	8.118 - degrees
	Total Depth	Surface length, DIB	0.712	0.601 - inch
Overgrown knot	Halfway-in length	Surface length, DIB	0.392	0.469 - inch
	Halfway-in width	Surface length, DIB	0.482	0.240 - inch
	Rake angle	Surface rise, length, DIB	0.386	8.156 - degrees
	Total Depth	DIB, surface width	0.810	0.366 - inch
Heavy distortion	Halfway-in length	Surface width, DIB	0.438	0.319 - inch
	Halfway-in width	Surface width, DIB	0.427	0.221 - inch
	Rake angle	--	N.S	--
	Total depth	DIB	0.799	0.417 - inch
	Clear area above	--	N.S	--
Medium distortion	Halfway-in length	DIB, surface width	0.336	0.257 - inch
	Halfway-in width	Surface width, DIB	0.329	0.163 - inch
	Rake angle	--	N.S	--
	Total depth	Surface width, length, DIB	0.822	0.362 - inch
	Clear area above	Surface rise, DIB	0.206	0.764 - inch
Light distortion	Halfway-in length	--	N.S	--
	Halfway-in width	Surface length	0.220	0.176 - inch
	Rake angle	--	N.S	--
	Total depth	DIB, surface width, length	0.775	0.334 - inch
	Clear area above	--	N.S	--

Table 3. –Statistics of the simulation of our defect detection system

Number of defects to be detected / Defect Type	Expected		Unexpected		Grand Total		False
	Total	Detected	Total	Detected	Total	Detected	
Knobs	32	28	34	6	66	34	
Sawn knots	19	19	19	2	38	21	
Others	8	1	50	3	58	4	
All Types	59	48	103	11	162	59	14

Figure 1.—Photo series showing processed defect sample

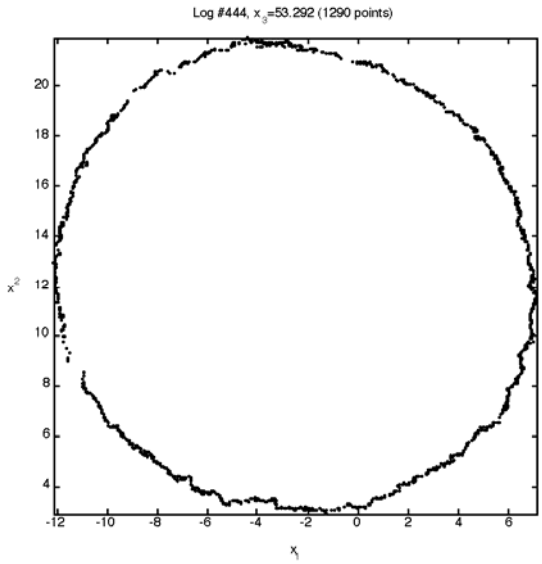

Figure 2.—A data cross-section representing the circumference of a log on a 2-D plane

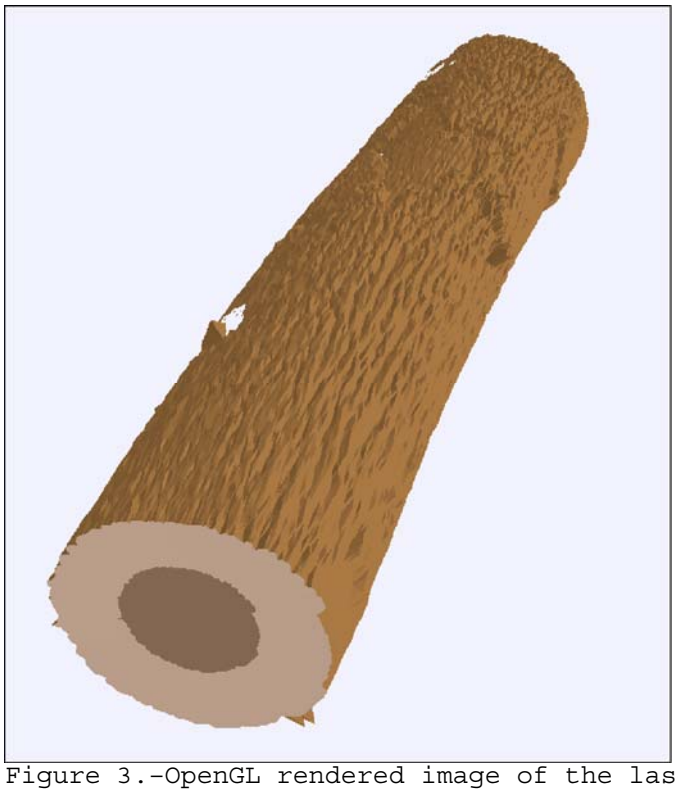

Figure 3.-OpenGL rendered image of the laser scanned log data

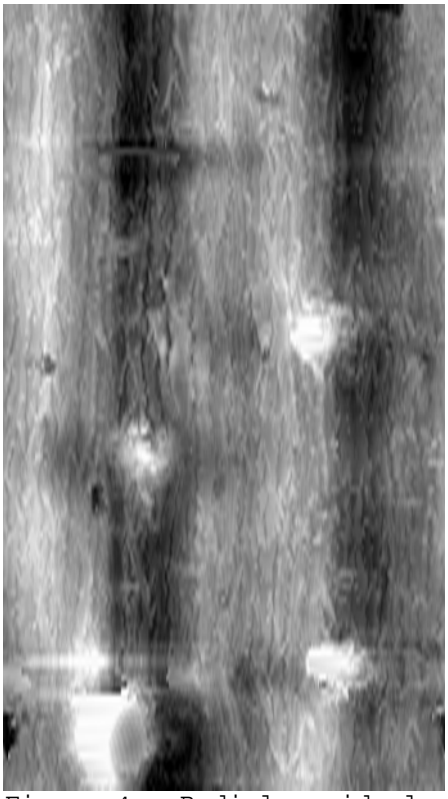

Figure 4.- Radial residuals generated by the log-unrolling process presented as a gray-level image. Light pixels represent protrusions from the log surface; dark pixels represent depressions. This log is approximately 9 feet long with a diameter of 2 feet.

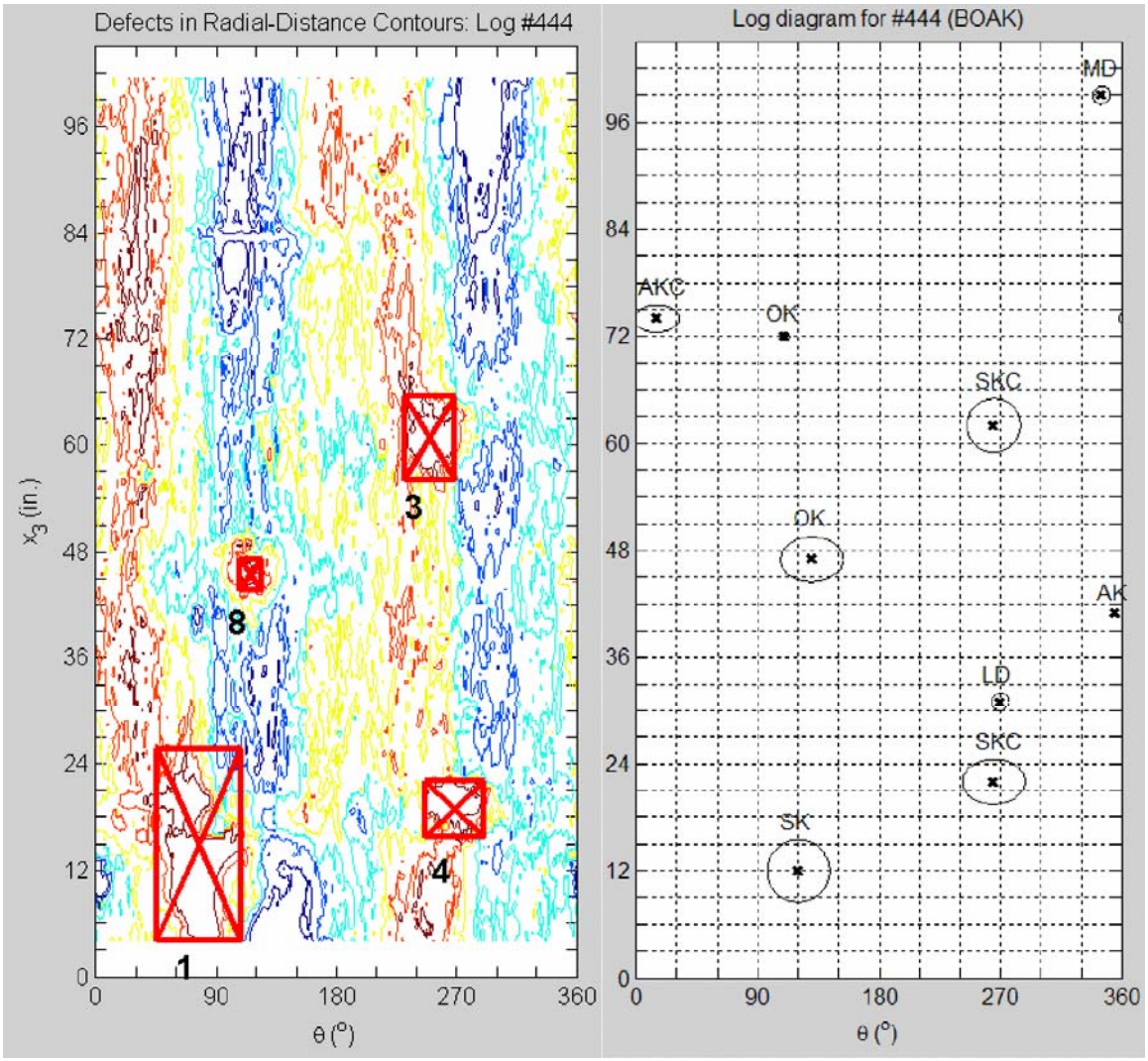

Figure 5.—Left: Contour plot of a log surface with the four most obvious defect areas marked with crossed rectangles labeled in the descending order of area size. Right: Defect diagram illustrating the "ground truth." Note that only five small and/or flat defects were not detected. Both plots were automatically generated by our programs.